Pyroelectric Polyelectrolyte Brushes

*Jian Wang,[1] Fei Hu,[1] Sabrina Sant,[1] Kanghyun Chu,[2] Lukas Riemer,[2] Dragan Damjanovic,[2] S. Michael Kilbey II,[3] and Harm-Anton Klok[1]**

1. Institut des Matériaux et Institut des Sciences et Ingénierie Chimiques, Laboratoire des Polymères, École Polytechnique Fédérale de Lausanne (EPFL), Bâtiment MXD, Station 12, CH-1015 Lausanne, Switzerland.

2. Group for Ferroelectrics and Functional Oxides, Institute of Materials, École Polytechnique Fédérale de Lausanne (EPFL), CH-1015 Lausanne, Switzerland.

3. Department of Chemistry, University of Tennessee, Knoxville, Tennessee 37996, United States.

Author Information:
Jian Wang: jw777@illinois.edu, ORCID: 0000-0003-0459-5833
Fei Hu: fei.hu@epfl.ch, ORCID: 0000-0001-5996-8524
Sabrina Sant: sabrina.sant@epfl.ch, ORCID: 0009-0000-1905-3426
Kanghyun Chu: kanghyun.chu@unibe.ch, ORCID: 0000-0003-2569-7644
Lukas Riemer: lukas.riemer@gmx.de, ORCID: 0000-0002-9817-090X
Dragan Damjanovic: dragan.damjanovic@epfl.ch, ORCID: 0000-0002-9596-7438
S. Michael Kilbey II: mkilbey@utk.edu, ORCID: 0000-0002-9431-1138
Harm-Anton Klok: harm-anton.klok@epfl.ch, ORCID: 0000-0003-3365-6543

Conflict of interest
The authors declare no conflict of interest.

CORRESPONDING AUTHOR: Email: harm-anton.klok@epfl.ch; Phone: + 41 21 693 4866

ABSTRACT

Piezo- and pyroelectric materials are of interest, for example, for energy harvesting applications, for the development of tactile sensors, as well as neuromorphic computing. This study reports the observation of pyro- and piezoelectricity in thin surface-attached polymer brushes containing zwitterionic and electrolytic side groups that are prepared via surface-initiated polymerization. The pyro- and piezoelectric properties of the surface-grafted polyelectrolyte brushes are found to sensitively depend on and can be tuned by variation of the counterion. The observed piezo- and pyroelectric properties reflect the structural complexity of polymer brushes, and are attributed to a complex interplay of the non-uniform segment density within these films, together with a non-uniform distribution of counterions and specific ion effects. The fabrication of thin pyroelectric films by surface-initiated polymerization is an important addition to the existing strategies towards such materials. Surface-initiated polymerization, in particular, allows for facile grafting of polar thin polymer films from a wide range of substrates via a straightforward two-step protocol that obviates the need for multistep laborious synthetic procedures or thin film deposition protocols. The ability to produce polymer brushes with piezo- and pyroelectric properties opens up new avenues of application of these materials, for example, in energy harvesting or biosensing.

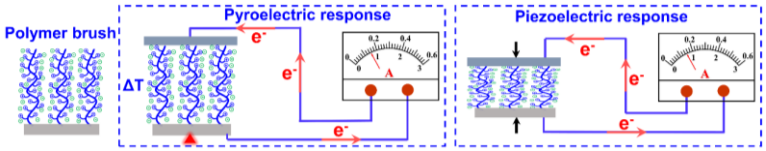

Explanation of TOC: Polyelectrolyte brushes prepared via surface-initiated polymerization display pyro- and piezoelectric behavior. These properties are attributed to the structural complexity of polymer brushes, and depend on, and can be tuned by variation of the counterion. The ability to produce polymer brushes with piezo- and pyroelectric properties opens new avenues of application of these materials, for example, in energy harvesting or biosensing.

Keywords: polyelectrolyte brushes, piezoelectricity, pyroelectricity, counterions, energy conversion, Hofmeister series.

INTRODUCTION

Polar materials are materials that possess an overall dipole moment.[1] Such materials are interesting since the polar order may impart properties such as piezo-, pyro-, and ferroelectricity. Materials with piezo-, pyro- and ferroelectric properties are of interest, for example, for energy harvesting applications, for the development of tactile sensors, as well as neuromorphic computing.[2]

There are a variety of inorganic oxides that possess polar materials properties.[3] These materials are characterized by a non-centrosymmetric crystal structure. While they possess outstanding piezo-, pyro-, and ferroelectric properties, inorganic materials also have a number of limitations. In particular, they can be challenging to process and have mechanical properties that are not well suited for applications where more pliable materials are required. In addition to hard, inorganic materials, however, there is also a variety of soft, polymeric materials that display piezo-, pyro- and ferroelectricity.[2b],[4] In contrast to their inorganic counterparts, polymers can be processed at low temperatures, are characterized by a low density, and have mechanical properties that make them attractive for the fabrication of flexible devices.[5] Examples of polymers that possess piezo-, pyro- or ferroelectric properties include synthetic polymers, most notably poly(vinylidene fluoride) (PVDF) and its copolymers,[6] as well as biopolymers such as cellulose and various proteins (including collagen and actin, amongst others).[4] Piezoelectric thin polymer films have also been prepared by surface grafting helical polypeptides.[7] The polar materials properties of piezo-, pyro-, and ferroelectric polymers originate from molecular dipoles that are organized in a non-centrosymmetric fashion.

Non-centrosymmetric polymer materials with polar order can also be prepared via supramolecular approaches.[8] Examples include the self-assembly of supramolecular inclusion complexes[9] or rod-coil molecules,[10] electrostatic layer-by-layer self-assembly[11] as well as blending of ABC triblock and AC diblock copolymers.[12] In addition to the fact that many of

these approaches use complex oligomeric or polymeric building blocks that require multistep synthesis, the polar order in these self-assembled materials is the result of weak, non-covalent interactions. While on the one hand this may be advantageous, as it potentially allows access to reversible and switchable properties, it may also limit the robustness and durability of the materials.

This report discusses the observation of pyro- and piezoelectricity in thin surface-attached polymer brush films containing zwitterionic or electrolytic side chains prepared via surface-initiated polymerization. The polar materials properties of these brushes are found to sensitively depend on and can be tuned by variation of the counterion. The observed piezo- and pyroelectric properties reflect the inherent structural complexity of polymer brushes, and are attributed to an intricate interplay of the non-uniform segment density of these films, together with a non-uniform distribution of counterions and specific ion effects. The ability to produce thin piezo-, and pyroelectric films by surface-initiated polymerization is an important addition to the other, existing strategies towards such materials. Since surface-initiated polymerization reactions can be performed at ambient temperature and atmosphere (i.e. without the need for degassing) to produce polymer brush coatings covering surface areas of several square meters within one hour,[13] this technology provides a facile route to graft polar thin polymer films from a wide range of substrates via a straightforward two-step process that obviates the need for multistep laborious synthetic procedures or thin film deposition protocols.

EXPERIMENTAL SECTION

Materials. All chemicals were used as received unless described otherwise. Copper(I)chloride (99.999%), copper(II)chloride (99.999%), copper(II)bromide (99.999%), copper(I)bromide (> 99.995%), 2,2'-bipyridyl (bpy) (99%), 2-bromo-2-methylpropionyl bromide, [2-(methacryloyloxy)ethyl]trimethylammonium chloride (METAC) solution 80 wt% in H_2O, *tert*-

butyl methacrylate (tBMA) (98%), 2-hydroxyethyl methacrylate (HEMA) (97%), ethanol (99.8%), basic aluminum oxide and 2-methacryloyloxyethyl phosphorylcholine (MPC, 97%) were purchased from Sigma Aldrich. Before use, MPC was washed with cold acetonitrile to remove the inhibitor, filtered and dried under vacuum. HEMA was freed from the inhibitor by passing through a column of activated, basic aluminum oxide, and distilled prior to use. Sodium bromide (ACS) was purchased from Acros. Sodium acetate (99%) was purchased from Abcr. Potassium thiocyanate (99%) was purchased from Fisher Scientific. Phosphate-buffered saline tablets (PanReac AppliChem) were purchased from ITW reagent. The ATRP initiator (6-(2-bromo-2-methyl)propionyloxy)hexyldimethylchlorosilane was synthesized as previously reported.[14] Dichloromethane was purchased from Fisher Chemicals. Methanol (MeOH) and sodium nitrate (98%) were purchased from Alfa Aesar. Isopropanol (99%) was purchased from Reactolab SA. Triethylamine was purchased from Aldrich and distilled over KOH before use. Dichloromethane (DCM) was purified and dried using a solvent purification system (PureSolv). Deionized water was obtained from a Millipore Direct-Q 5 water purification system. Pyroelectric measurements were performed on polymer brushes, which were grown from 0.8 cm × 1 cm rectangular fused silica substrates with a thickness of ~ 525 μm. Samples for piezoelectric force microscopy (PFM) and scanning Kelvin probe microscopy (SKPM) were grafted from 0.8 cm × 1 cm rectangular boron-doped silicon substrates with a thickness of ~ 525 μm. A poled poly(vinylidene fluoride) (PVDF) film (thickness ~ 50 μm) coated with a silver electrode was purchased from Entran, now TE Connectivity, and cut into 8 × 10 mm rectangular specimens.

METHODS. X-ray photoelectron spectroscopy (XPS) was carried out using an Axis Ultra instrument from Kratos Analytical equipped with a conventional hemispheric analyzer. The X-ray source employed was a monochromatic Al Kα (1486.6 eV) source operated at 100 W and

10^{-9} mbar. Surfaces were cleaned with a Femto O_2 Plasma system (200 W, Diener Electronic). Dry film thicknesses were determined using a SemiLAB (SE2000) ellipsometer, and calculated based on a four-layer silicon/silicon oxide/polymer brush/air model, assuming the polymer brush to be isotropic and homogeneous.

Swollen film thicknesses were measured at room temperature in PBS (pH = 7.4) using a liquid cell at an incident angle of 70°. The samples were allowed to equilibrate in the liquid cell for 30-60 seconds before measuring one spot per substrate. One measurement point per wafer was used for the experiments in liquid medium. The SEA software from SemiLAB was used to fit the raw data. For PMETAC brushes a gradient model with 2 sublayers was applied with the parabolic function $c(z) = a(z-z_0)^2 + c_0$, where a = -1.36659, c_0 = 1.06973, z_0 = -0.36726, and a refractive index n = 1.35608. Swollen film thicknesses of PMPC brushes were determined applying a single slab box model with a refractive index n = 1.367. Piezoelectric force microscopy (PFM) and scanning Kelvin probe microscopy (SKPM) experiments were carried out on a Cypher VRS AFM instrument (Oxford Instruments) using Pt-coated Si conductive tips (MikroMasch, NSC35). PFM measurements were performed in the single frequency out-of-plane mode with an AC driving voltage of 1 V, a frequency of 828819.9 Hz and a scan size 20 × 20 μm^2. For SKPM surface potential measurements, the AC driving voltage was 0.1 V with a frequency of 159500 Hz, a tip lifting height of 4 x 10^{-8} m, and a scan size of 30 × 30 μm^2 for PMETAC brushes, and of 20 × 20 μm^2 for poly((2-(methacryloyloxy)ethyl)trimethylammonium salt) brush samples in which the chloride counterion in the original PMETAC sample was exchanged for acetate, bromide, thiocyanate or nitrate. PFM and SKPM images were analyzed with Gwyddion, and the inverse piezoelectric displacement results are reported without further treatment. Spin coating was performed on a Convac ST 146 spin coater. Gel permeation chromatography (GPC) analysis was performed on a Polymer Laboratories PL-GPC 50 instrument equipped with PSS NOVEMA Max columns

(Ref: 212-0002) and a differential refractive index detector. The mobile phase was water (HPLC grade) with 200 mM acetic acid and 333 mM sodium acetate. Sample analysis was performed at 40 ºC at a flow rate of 1 mL/min. Samples were filtered prior to analysis and polymer molecular weights were analysed using narrow dispersity linear poly(ethylene glycol) standards with molecular weights ranging from 26,100 to 1,015,000 Da.

PROCEDURES

Preparation of ATRP initiator-modified boron-doped silicon and fused silica surfaces. Boron-doped silicon and fused silica surfaces were modified following a previously published protocol.[15]

Surface-initiated atom transfer radical polymerization of [2-(methacryloyloxy)ethyl]trimethylammonium chloride (METAC). Surface-initiated atom transfer radical polymerization of METAC was performed following a procedure based on earlier published protocols.[16] 2,2'-Bipyridyl (bpy) (351.4 mg, 2.25 mmol) and $CuCl_2$ (6.725 mg, 0.05 mmol) were dissolved in a mixture of an 80 wt% aqueous solution of METAC (15.6 g, 60 mmol) and isopropanol (12.5 mL). After three freeze/pump/thaw cycles, CuBr (178.75 mg, 1.25 mmol) was added under nitrogen flow. The molar ratio of METAC/CuBr/$CuCl_2$/bpy in the reaction mixture was 48 : 1: 0.04 : 1.8. The mixture was sonicated to completely dissolve the CuBr. After an additional freeze/pump/thaw cycle, the resulting ATRP solution was cannula transferred to a nitrogen purged flask containing the initiator-functionalized substrates. Surface-initiated ATRP was allowed to proceed at room temperature. After a pre-determined period of time, the substrates were removed from the ATRP solution, rinsed extensively with water and ethanol, and dried under a flow of N_2.

Counterion exchange. To exchange the chloride counterion for others, PMETAC brushes were immersed in a 0.2 M aqueous (MilliQ) solution of NaBr, $NaNO_3$, KSCN or CH_3COONa (NaAc) for 45 min.[17]

Surface-Initiated Atom Transfer Radical Polymerization of MPC,[15] tBMA[18] and HEMA[19] was carried out following established protocols.

Patterned Polymer Brushes. Patterned polymer brushes were prepared via surface-initiated polymerization from micropatterned substrates, which were obtained by UV irradiation of initiator modified silicon wafers using a TEM grid as a photomask.[18] A Hamamatsu (Lightningcure L8858, 200 W, wavelength = 360 nm) UV lamp was used as the light source and substrates were irradiated for 8 min at a lamp-to-substrate distance of 6 cm.

Solution Atom Transfer Radical Polymerization of METAC. Solution polymerization of METAC was performed following the protocol for the SI-ATRP of METAC with a slight modification. Instead of using initiator-modified substrates, (6-(2-bromo-2-methyl)propionyloxy)hexyldimethylchlorosilane (0.07 mL 0.24 mmol, monomer/initiator = 250 : 1) was used as an initiator, and was added to a mixture of METAC, isopropanol, $CuCl_2$ and bpy that had been degassed by three freeze-pump-thaw cycles. After polymerization at room temperature for 3 h, the polymer solution was passed through a column of neutral Al_2O_3. The polymer was precipitated in methanol and dried under vacuum overnight. GPC analysis of the polymer indicated M_n = 28 kDa and Đ = 1.37 (**Supporting Information Figure S1A**).

Solution Atom Transfer Radical Polymerization of MPC. Solution polymerization of MPC was performed following the protocol for the SI-ATRP of METAC with a slight modification.[15] Instead of using initiator-modified surfaces, (6-(2-bromo-2-methyl)propionyloxy)hexyldimethylchlorosilane (0.026 mL, 0.09 mmol, monomer/initiator = 250 : 1) was used as the initiator. Briefly, MPC (6.65 g, 22.5 mmol) was placed in a Schlenk tube under nitrogen atmosphere. The Schlenk tube was subsequently evacuated and filled with

nitrogen three times. Then, 2,2′-bipyridyl (bpy) (140.5 mg, 0.9 mmol), $CuBr_2$ (10.05 mg, 0.045 mmol), (6-(2-bromo-2-methyl)propionyloxy)hexyldimethylchlorosilane (0.026 mL, 0.09 mmol) and a methanol/water solution (4:1, v:v, 15 mL) were added into another Schlenk tube. After three freeze/pump/thaw cycles, the solution was frozen. Then, CuBr (64.5 mg, 0.45 mmol) was added under a nitrogen flow, and the frozen solution was thawed. The mixture was stirred under nitrogen and briefly sonicated to completely dissolve the CuBr. After an additional freeze/pump/thaw cycle, the resulting ATRP solution was cannula transferred to a Schlenk tube containing the MPC. After 15 h, the polymer solution was passed through a column of neutral Al_2O_3. The polymer was precipitated in methanol, and dried under vacuum overnight. GPC analysis revealed M_n = 70 kDa, and Đ = 1.31 (**Supporting Information Figure S1B**).

Dynamic Pyroelectric Measurements.[20] These measurements were performed in dynamic mode with an amplitude of ~ 4 K and a frequency of 10 mHz. The specimen was placed on a copper bottom electrode and contacted with a platinum top electrode. The temperature of the polymer brush samples was subjected to a triangular temperature modulation, which was generated with a feedback-controlled Peltier element placed below the bottom electrode. A photograph of this set-up is included in **Supporting Information Figure S2**. Currents were converted to voltage with a transimpedance amplifier circuit, and subsequently measured with a HP3478A multimeter (Hewlett Packard, Palo Alto, California, U.S.).

Statistical Analysis. Processing and analysis of ellipsometry data was performed as described above. Current amplitudes, piezoelectric responses and surface potentials are presented as mean ± standard deviation (s.d.) (n = 3). Data presented in **Figures S1** represent the result of a single (n = 1) GPC measurement. XPS spectra in **Figure S3** were deconvoluted using CasaXPS. No further statistical analyses or tests of significance were performed.

RESULTS AND DISCUSSION

Results. This manuscript reports the results of experiments that have investigated the polar materials properties, specifically the pyro- and piezoelectric response, of a series of thin polymer films prepared via surface-initiated polymerization. Such polymer films, which are commonly referred to as polymer brushes, are composed of polymer chains that are anchored via one end-group to a solid substrate.[21] For this study, 4 different polymer brush samples were studied, which were prepared via surface-initiated atom transfer radical polymerization (SI-ATRP) (**Scheme 1**). The polymer brush films studied included a strong polyelectrolyte brush, viz. poly((2-(methacryloyloxy)ethyl)trimethylammonium chloride) (PMETAC), a zwitterionic polymer brush (poly(2-methacryloyloxyethyl phosphorylcholine), (PMPC)), as well as a non-charged hydrophobic poly(*tert*-butyl methacrylate) (PtBMA) brush, and a non-charged hydrophilic poly(2-hydroxyethyl methacrylate) (PHEMA) brush. These polymer brush films were grown from fused silica or boron-doped silicon substrates, which were modified with (6-(2-bromo-2-methyl)propionyloxy)hexyldimethylchlorosilane as the initiator, via SI-ATRP following published protocols.[15,16,18] The experiments described in this report were performed with polymer brush samples with dry film thicknesses of 100 - 150 nm, as measured via ellipsometry. XPS spectra that confirm the chemical composition of the PMETAC brushes are included in **Supporting Information Figure S3**. PMPC, PHEMA and PtBMA brushes were prepared and characterized as reported in earlier publications.[15, 18] Grafting densities of the polymer brushes were estimated from the swelling ratios of the different samples (obtained from the swollen and dry film thicknesses determined by ellipsometry) following the Milner-Witten-Cates model (**Supporting Information Table S1**).[22] The PMETAC, PMPC, PHEMA and PtBMA brushes investigated in this study have grafting densities of 0.13 ± 0.005 chains/nm^2, 0.16 ± 0.016 chains/nm^2, 0.54 ± 0.068 chains/nm^2 and 0.15 ± 0.008 chains/nm^2.

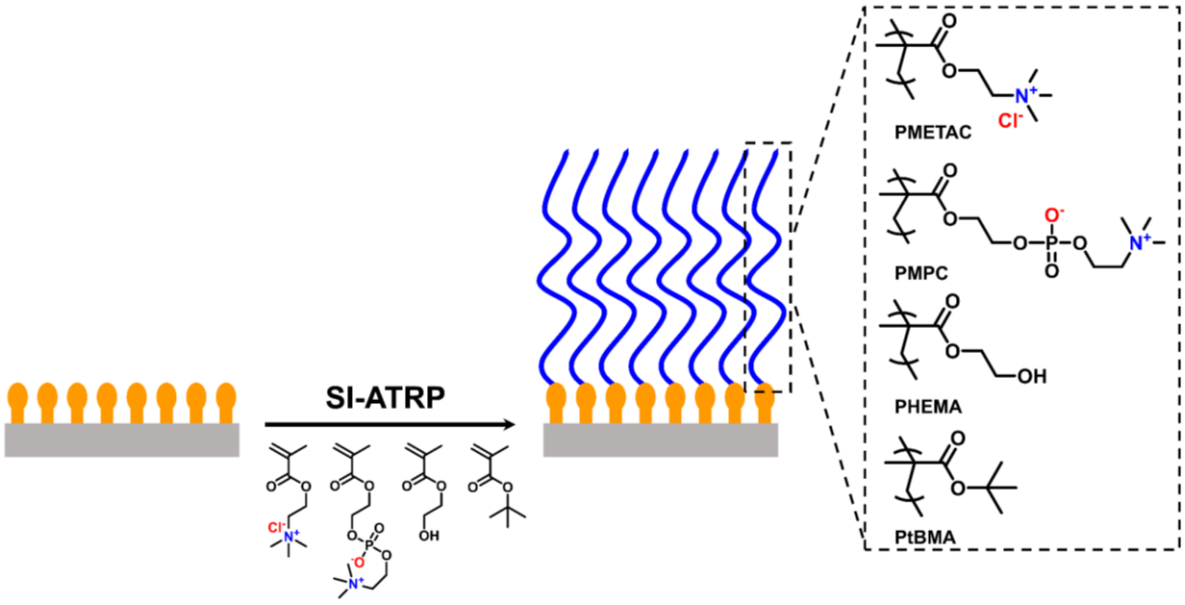

Scheme 1. Preparation of PMETAC, PMPC, PHEMA and PtBMA brushes via SI-ATRP.

In a first set of experiments, the pyroelectric properties of the brush samples were evaluated using the set-up illustrated in **Figure 1A**. For these experiments, the temperature of the polymer brushes was varied from 19.5 to 23.5 °C by heating and cooling following a sawtooth pattern with a frequency of 10 mHz, and the current was measured in real-time. While a pyroelectric current was observed for the PMETAC brush, which contains chloride counterions, and the zwitterionic PMPC brush (**Figure 1B** and **Figure 1C**, respectively), the neutral PHEMA and PtBMA brushes did not show a pyroelectric response (**Figure 1D** and **Figure 1E**). For the PMETAC sample an average current amplitude of ~ 2.37 pA was recorded, as compared to ~ 0.85 pA for the PMPC sample (**Supporting Information Figure S4**). Comparison of **Figure 1B** and **Figure 1C** also reveals that while the current and temperature alternations are in phase for the PMETAC sample, these two signals are out of phase for the PMPC brush. The non-zero current that is seen in **Figure 1D** and **Figure 1E** is the background current in the electronic circuit that is used to measure the pyroelectric properties.[20] In a long-term experiment that covered a period of 16 h, the pyroelectric current amplitude of the PMETAC brush was found to decrease from 2.37 pA to 0.9 pA over the first 2000 s, and then remained constant

(**Supporting Information Figure S5**). Furthermore, dynamic pyroelectric measurements on a PMETAC brush sample directly after synthesis, and subsequently again after leaving the same sample for a week under ambient air and temperature revealed a similar response, indicating that storage of the polymer brush films does not significantly influence the pyroelectric properties (**Supporting Information Figure S6**). The triangular pyroelectric response of the PMETAC and PMPC brushes is markedly different from that observed for well-known pyroelectric inorganic oxides,[20, 23] or pyroelectric polymers such as poly(vinylidene fluoride) (PVDF), which is characterized by a pyroelectric response that resembles a square wave function. To highlight this difference, **Supporting Information Figure S7** presents the pyroelectric current response measured using the set-up illustrated in **Figure 1A** for a ~ 50 μm thick commercially available PVDF film, both freestanding as well as placed on a fused silica substrate. Careful inspection of the results of the PMETAC brush presented in **Figure 1B** reveals that the pyroelectric current response is not purely triangular, but shows a gradual plateauing of the current as it approaches its maximum value, which suggests that the polarization of the sample is not constant under the conditions of the applied temperature oscillation. This may indicate that the kinetics of polarization of the brush films are slow as compared to e.g. PVDF. A pyroelectric response similar to that observed for PMETAC and PMPC brushes (**Figure 1B** and **Figure 1C**, respectively) has also been reported for polycrystalline aggregate films of the protein lysozyme.[24]

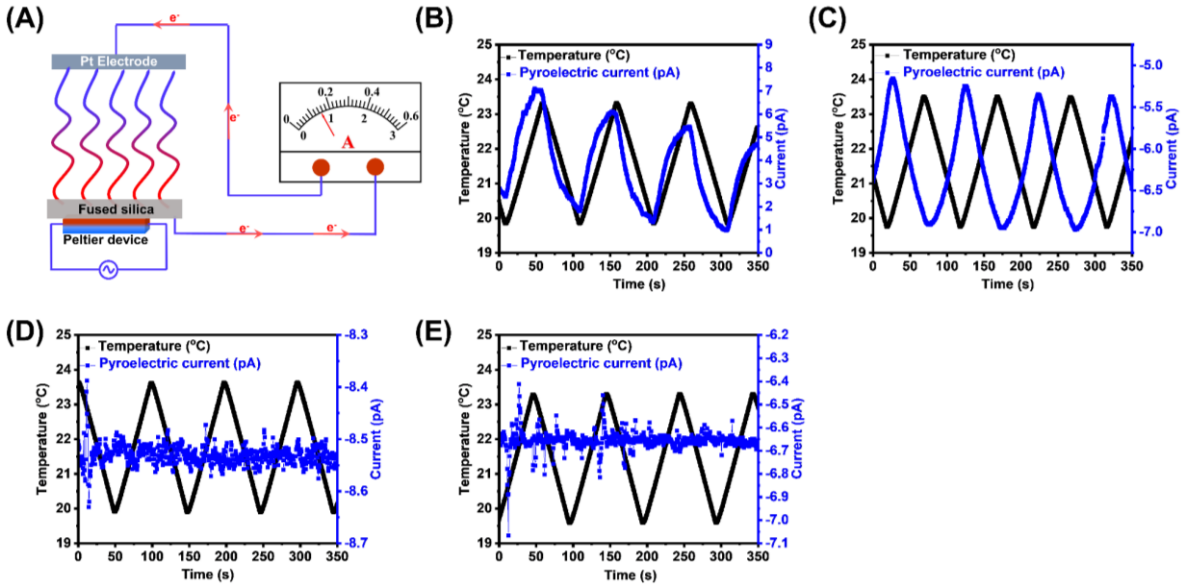

Figure 1. (A) Schematic illustration of the setup that was used to probe the dynamic pyroelectric properties of the brushes. Sample temperature and current response for dynamic pyroelectric analysis of (B) a PMETAC brush containing chloride counterions with a dry film thickness of 100 nm, (C) a zwitterionic PMPC brush with a dry film thickness of 100 nm, (D) a neutral hydrophilic PHEMA brush with a dry film thickness of 100 nm and (E) a neutral hydrophobic PtBMA brush with a dry film thickness of 150 nm.

Next, in a series of control experiments, the dynamic pyroelectric properties of a pristine fused silica substrate, an ATRP initiator modified fused silica substrate, as well as of spin coated films of solution synthesized PMETAC and PMPC with thicknesses of 80 and 100 nm were evaluated (**Figure 2**). The characterization of spin coated PMETAC and PMPC films with thicknesses comparable to that of the surface-grafted polymer brushes prepared via SI-ATRP allows to study the effect of chain conformation of the pyroelectric properties. No alternating current was measured on the bare and initiator-modified silica substrates, and on the spin coated PMPC film. The spin coated PMETAC film did show a pyroelectric response, however, the observed current amplitude (< 0.15 pA) was much smaller as compared to that measured on the corresponding brush sample (2.37 pA).

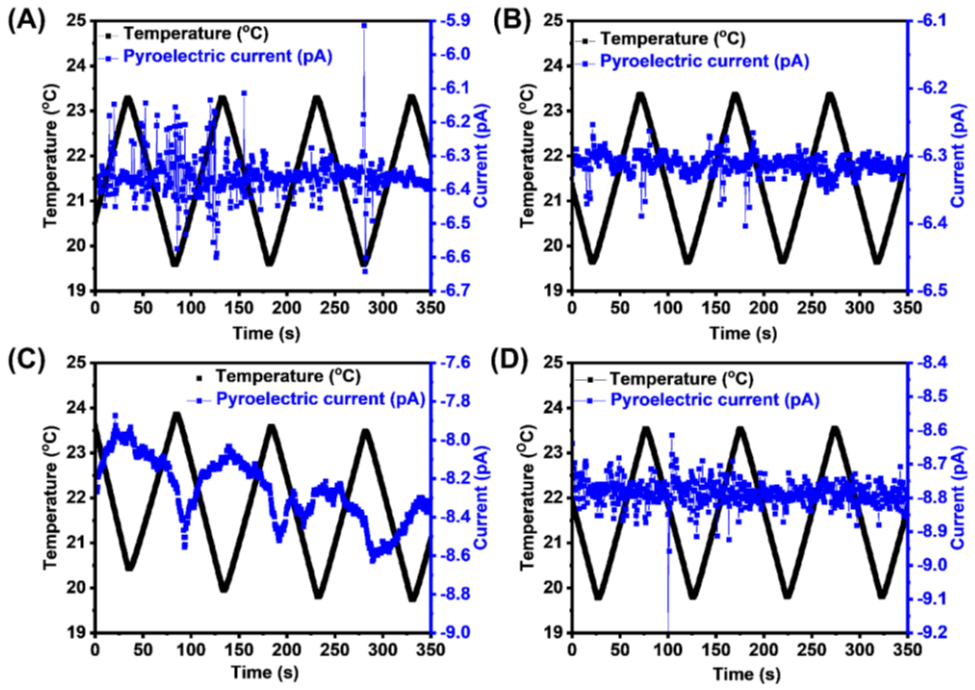

Figure 2: Sample temperature and current response for dynamic pyroelectric analysis of (A) a pristine fused silica substrate, (B) an ATRP initiator modified fused silica substrate, (C) a spin coated PMETAC film with a film thickness of 80 nm and (D) a spin coated PMPC film with a film thickness of 100 nm.

Via counterion exchange with NaBr, $NaNO_3$, KSCN and CH_3COONa (NaAc), poly((2-(methacryloyloxy)ethyl)trimethylammonium salt) brush samples were obtained in which the chloride counterion in the original PMETAC sample was exchanged for acetate, bromide, nitrate or thiocyanate. **Supporting Information Figure S8** presents survey XPS spectra of the original PMETAC brush, and of the corresponding counterion exchanged poly((2-(methacryloyloxy)ethyl)trimethylammonium salt) brush samples, which indicate complete replacement of the original chloride counterion with acetate, bromide, thiocyanate and nitrate counterions. **Figure 3A – Figure 3E** compare the pyroelectric response of the original PMETAC brush with that of the corresponding acetate, bromide, nitrate and thiocyanate salt forms. While for the original PMETAC brush a current amplitude of 2.37 pA was measured, the response decreased to 1.89, 0.72, 0.19 and 0.09 pA after exchanging the chloride

counterions for acetate, bromide, thiocyanate and nitrate anions (**Figure 3F**). The results presented in **Figure 3** show that counterion exchange does not only influence the pyroelectric current, but can also lead to a shift in the phase between the temperature alternation and current response (this is most prominent for the acetate and bromide counterion exchanged samples, see **Figure 3A** versus **Figure 3B** and **Figure 3C**). Comparison of **Figure 3D** and **Figure 3E** with **Figure 3A** furthermore suggests a change from a triangular to a more square wave response.

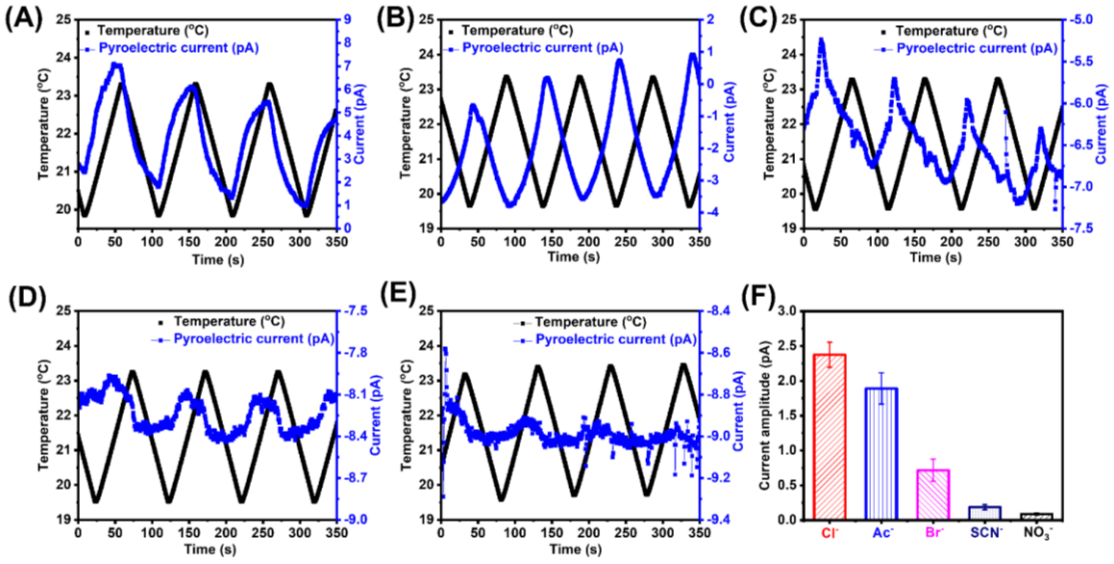

Figure 3: Sample temperature and current response for dynamic pyroelectric analysis of (A) a PMETAC brush (d = 100 nm – same as **Figure 1B**), and poly((2-(methacryloyloxy)ethyl)trimethylammonium salt) brush samples in which the chloride counterion in the original PMETAC sample is exchanged for (B) acetate, (C) bromide, (D) thiocyanate or (E) nitrate; (F) Pyroelectric current amplitude of a 100 nm thick PMETAC brush and the corresponding counterion-exchanged poly((2-(methacryloyloxy)ethyl)trimethylammonium salt) brush samples. The error bars represent the standard deviation of three cycles of current amplitudes.

Since pyroelectric materials are also piezoelectric, several polymer brush samples were also studied by piezoelectric force microscopy (PFM) to assess their inverse piezoelectric response. **Figure 4** summarizes the results from PFM experiments on PMETAC, PMPC and PHEMA brushes. Analysis of PMETAC and PMPC brushes with dry film thicknesses of 110 nm and 100 nm revealed an inverse piezoelectric displacement of 40 pm and 7 pm, respectively, at 20 °C when subjected to a driving voltage of 1 V (**Figure 4A** and **Figure 4B**). In contrast, no obvious piezoelectric response was observed for the PHEMA brush sample (**Figure 4C**). The outcomes of these experiments are consistent with the results of the dynamic pyroelectric measurements that are summarized in **Figure 1**. The results of the PFM analysis of the poly((2-(methacryloyloxy)ethyl)trimethylammonium salt) brush samples in which the chloride counterion in the original PMETAC samples was exchanged for acetate, bromide, nitrate or thiocyanate are summarized in **Supporting Information Figure S9**. While no significant change in piezoelectric response was observed upon exchanging the chloride to acetate counterions, the piezoelectric response decreased from 38 pm to 8 pm, 8 pm and 10 pm, when chloride was exchanged for bromide, thiocyanate and nitrate, respectively. The counterion effect on the piezoelectric response of the poly((2-(methacryloyloxy)ethyl)trimethylammonium salt) brushes (**Supporting Information Figure S10**) follows a trend that is similar to that observed for the current amplitude in the dynamic pyroelectric measurements (**see Figure 3F**). The counterion effects that were observed when the pyro- and piezoelectric properties of the PMETAC brushes were studied, were corroborated by scanning Kelvin probe microscopy (SKPM) experiments, which probe the surface charge of the brushes (**Supporting Information S11**). These experiments revealed a decrease of the surface charge of the poly((2-(methacryloyloxy)ethyl)trimethylammonium salt) brushes upon exchanging the original chloride counterion for acetate, bromide, thiocyanate and nitrate, with a counterion dependence that resembles those illustrated in **Figure 3F** and **Supporting Information S10**.

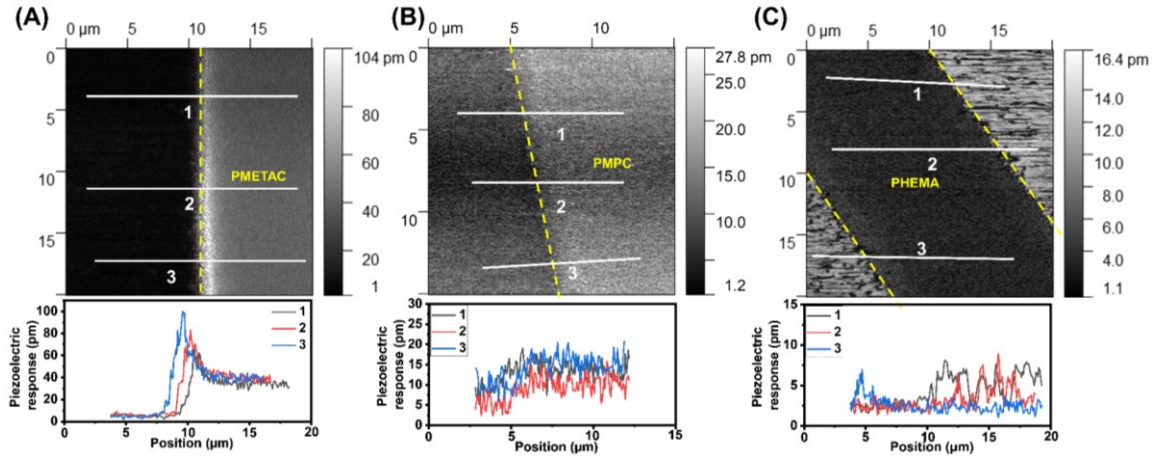

Figure 4. PFM piezoresponse amplitude of (A) a PMETAC brush with a dry film thickness of 110 nm; (B) a PMPC brush with a dry film thickness of 100 nm and (C) a PHEMA brush with a dry film thicknesses of 100 nm measured at 20 °C with a driving voltage of 1 V. The white lines in the images (1, 2, and 3) represent the cross-sectional profiles that are shown in the panels underneath each of the images.

Discussion. The observations reported above reflect the structural complexity of surface-grafted polymer brush films and highlight the importance of ion-specific behavior. Qualitatively, we hypothesize that the pyro- and piezoelectric response of the polymer brush films examined in this study can be rationalized considering two interrelated effects, which are schematically illustrated in **Figure 5**.

1) Polymer brush films are characterized by a non-uniform dielectric profile that varies along the direction perpendicular to the substrate. Surface-initiated polymerization produces assemblies of chain end-tethered polymers with conformations that are stretched in the direction normal to the surface, and that are essentially devoid of translation in lateral direction. While the extent of stretching is strongest when the chains are in a good solvent, even in the melt state end-tethering necessarily results in chain stretching to alleviate lateral crowding enforced by the covalent linking to the surface. Augmented by effects such as the chain length heterogeneity

(i.e. dispersity) of the surface-grafted polymer chains, the extent of chain stretching for a single polymer graft decreases in the direction away from the substrate. The result of this is a non-uniform monomer segment density profile, and coupled with that, for polyelectrolyte brushes a non-uniform counterion (and thus charge distribution), which results in a locally varying dielectric environment.[25] While the extent of chain stretching is strongest, and concomitantly the resulting non-uniformity in monomer segment density and counterion distribution most prominent, in a solvent swollen brush, even in the absence of significant solvent or in the dry state, such as the brushes studied here, the end-tethering of the polymer grafts will enforce chain stretching and result in a non-uniform segment density profile and counterion distribution (which will be particularly prominent at the brush – air interface). As a consequence of the local variation of the dielectric environment, the strength of any dipole within the polymer brush film will depend on its location within the polymer film, and vary in the direction normal to the confining surface (i.e. going from the substrate – polymer brush to the polymer brush – air interface).

2) Counterion distribution and specific ion effects. Counterions in a polyelectrolyte brush can be considered either as "bound" counterions, which are condensed to the polymer backbone and generate an electrical dipole, or as "free" counterions.[26] Small angle x-ray scattering[27] and anomalous x-ray reflectivity[28] experiments on solvent swollen polymer brushes, in combination with theoretical predictions[29] have shown that counterions are non-uniformly distributed within polyelectrolyte brushes, and are typically at higher concentration in proximity of the substrate – brush interface. As a consequence of the non-uniform dielectric constant of the polymer brush layer, the strength of the electrical dipoles generated by the condensed ion pairs will vary across the film in the direction normal to the surface, resulting in an overall non-centrosymmetry in the direction perpendicular to the polymer brush - substrate interface (the experimental data do not allow to draw conclusions as to the direction of

orientation of the vector that characterizes this non-centrosymmetry). The non-centrosymmetry of the polymer brush films, and the resulting polar materials properties will sensitively depend on the nature of the counterion. The effects of varying the nature of the counterion may not be trivial, and are intricate (and thus a challenge to resolve experimentally), but could include effects on the strength of the electrical dipoles, as well as the counterion distribution in the polymer brush film. Such specific ion effects, often also referred to as the Hofmeister series, remain largely elusive, in particular in non-aqueous media.[30] In what follows below, the contributions of these effects to the pyro- and piezoelectric properties of the polymer brushes examined in this study will be discussed.

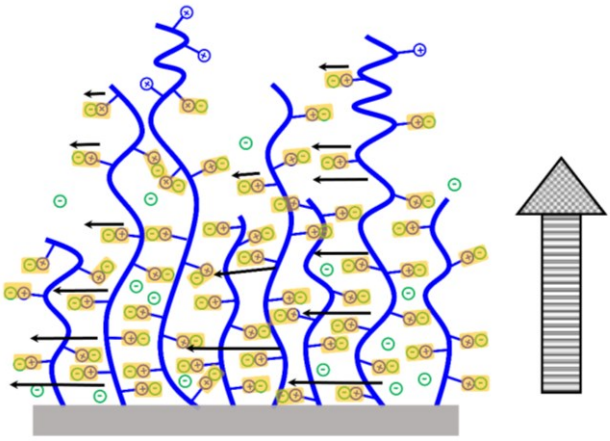

Figure 5: Schematic illustration of a chain-end tethered polyelectrolyte brush. The cartoon serves to highlight the non-uniform counterion distribution as well as the variation of the strength of ionic dipoles in the direction perpendicular to the substrate, which are suggested to contribute to the non-centrosymmetric character (indicated by the shaded vector in the cartoon) of these films, and their pyro- and piezoelectric properties. The direction of the vector is for illustrative purposes only. The experimental data do not allow to conclude whether this vector is directed away from, or pointing towards, the substrate.

The PMPC brushes investigated in this study contain electrical dipoles that are generated by the spatially separated, positively charged ammonium groups and the negatively charged phosphate groups that are incorporated in the side chains of the polymer grafts. These positively charged ammonium groups and the negatively charged phosphate groups are covalently linked together, and as a consequence there are no free, unbound counterions in these films. Since the dielectric constant of the brush varies in the direction perpendicular to the substrate, the strengths of the electrical dipoles will also change going from the substrate – brush interface to the polymer brush - air interface, resulting in a non-centrosymmetric dielectric environment (in the direction normal to the surface) within PMPC brush film, which is then reflected in the observed pyro- and piezoelectric responses of these films. The absence of a pyroelectric response in the spin coated PMPC film (**Figure 2D**) highlights the impact of the non-uniform structure of polymer brushes that is imparted as a consequence of the chain-end anchored architecture of these thin films.

In the PMETAC brush films, electrical dipoles can be formed between the positively charged ammonium groups and bound, negatively charged chloride counterions. The pyro- and piezoelectric response observed for these brushes reflects the effects mentioned above, i.e. a non-uniform monomer segment distribution and locally varying dielectric function in the direction normal to the surface through the brush, as well as a non-uniform counterion distribution. The counterion dependent surface charges that were observed by SKPM analysis of the poly((2-(methacryloyloxy)ethyl)trimethylammonium salt) brushes (**Supporting Information Figure S11**) reflect the differences in counterion and charge distribution between these various polyelectrolyte brushes. The decrease in pyroelectric current that is observed during analysis of a PMETAC brush over a period of 16 h, may suggest the establishment of a stable or “equilibrium” counterion distribution or concentration gradient as a pristine (i.e. non-

equilibrated sample) is exposed to a sawtooth-type temperature modulation process for a longer period of time. The effect of the non-uniform segment density and locally varying dielectric function is reflected in the dynamic pyroelectric measurements on spin coated PMETAC films, which reveal a 5-fold decrease in the current amplitude as compared to the PMETAC brush samples (**Figure 2C**). As the pyroelectric measurements on the counterion exchanged brushes highlight, the properties of the poly((2-(methacryloyloxy)ethyl)trimethylammonium salt) brushes are very sensitive to the nature of the counterion. As mentioned above, varying the counterion will not only impact the strength of the electrical dipole, but may also change counterion distribution, which both have an influence on the polar materials properties of the polymer brushes. The results presented in **Figure 3** highlight that counterion exchange not only influences the magnitude of the pyroelectric current, but also the phase of the response, which reflects the direction of polarization, as well as the type of response (i.e. triangular versus square wave). The trend in the data presented in **Figure 3F** is reminiscent of a Hofmeister series type trend, however, with a reversal of Cl^- and acetate, and of NO_3^- and SCN^-. It is interesting to compare the pyro- and piezoelectric response of the PMETAC brushes, and in particular the effect of the counterions, with the results of experiments that have probed the interaction between this brush and Hofmeister ions using QCM-D and ellipsometry experiments.[31] This earlier work revealed that the more chaotropic SCN^- and NO_3^- ions interacted stronger with the (chaotropic) quaternary ammonium groups of the PMETAC brushes, as opposed to Cl^- and acetate, which are at the border between chaotropic and kosmotropic in the Hofmeister series. This may indicate that poly((2-(methacryloyloxy)ethyl)trimethylammonium salt) brushes with more chaotropic counterions incorporate fewer mobile ions as compared to brushes with more kosmotropic counterions. As a consequence, the nature of the counterion may also impact the counterion distribution in polymer brush films. While the QCM-D and ellipsometry experiments reported earlier in the literature were done on polymer brushes immersed in liquid,

and the pyro- and piezoelectric characterization reported here was conducted on dry brush films under ambient conditions, many of the same factors that impact the strength of ionic interactions and ion distribution may be at play.

CONCLUSIONS

The results presented in this article demonstrate that surface-initiated polymerization can be used to produce polyelectrolyte brushes that display pyro- and piezoelectric properties. The pyro- and piezoelectric properties of the polyelectrolyte brushes were found to sensitively depend on and could be tuned by variation of the counterion, and are attributed to the structural complexity of these thin films, most notably their non-uniform segment density profiles, in combination with a non-uniform counterion distribution and ion specific effects. The observation of pyro- and piezoelectricity in surface-grafted polymer brush films produced via surface-initiated polymerization is attractive as it opens up new and straightforward pathways towards generating thin polymer films with polar materials properties.

AUTHOR INFORMATION

Jian Wang: jw777@illinois.edu, ORCID: 0000-0003-0459-5833

Fei Hu: fei.hu@epfl.ch, ORCID: 0000-0001-5996-8524

Sabrina Sant: sabrina.sant@epfl.ch, ORCID: 0009-0000-1905-3426

Kanghyun Chu: kanghyun.chu@unibe.ch, ORCID: 0000-0003-2569-7644

Lukas Riemer: lukas.riemer@gmx.de, ORCID: 0000-0002-9817-090X

Dragan Damjanovic: dragan.damjanovic@epfl.ch, ORCID: 0000-0002-9596-7438

S. Michael Kilbey, II: mkilbey@utk.edu, ORCID: 0000-0002-9431-1138

Harm-Anton Klok: harm-anton.klok@epfl.ch, ORCID: 0000-0003-3365-6543

ACKNOWLEDGMENTS

This work was financially supported by the China Scholarship Council (No. 201506360078 to JW, and No. 202006240050 to FH). SMK acknowledges support from the National Science Foundation (award #2204396).

CONFLICT OF INTEREST

The authors declare no conflict of interest.

DATA AVAILABILITY STATEMENT

The data that support the findings of this study are available from the corresponding author upon reasonable request.

REFERENCES

[1] S. T. Lagerwall, in *Encyclopedia of Materials: Science and Technology (Second Edition)* (Ed.: K. H. J. Buschow, R. W. Cahn, M. C. Flemings, B. Ilschner, E. J. Kramer, S. Mahajan, P. Veyssière,), Elsevier, **2001**, pp. 3044-3063.

[2] a) M. Smith, S. Kar-Narayan, *Int. Mater. Rev.* **2022**, *67*, 65-88; b) M. Abbasipour, R. Khajavi, A. H. Akbarzadeh, *Adv. Eng. Mater.* **2022**, *24*, 2101312; c) X. Niu, B. Tian, Q. Zhu, B. Dkhil, C. Duan, *Appl. Phys. Rev.* **2022**, *9*, 021309.

[3] a) P. S. Halasyamani, K. R. Poeppelmeier, *Chem. Mater.* **1998**, *10*, 2753-2769; b) E. Wachtel, I. Lubomirsky, *Adv. Mater.* **2010**, *22*, 2485-2493.

[4] a) H. Kaczmarek, B. Królikowski, E. Klimiec, M. Chylińska, D. Bajer, *Russian Chemical Reviews* **2019**, *88*, 749; b) R. G. Kepler, R. A. Anderson, *Advances in Physics* **1992**, *41*, 1-57; c) T. D. Usher, K. R. Cousins, R. Zhang, S. Ducharme, *Polym. Int.* **2018**, *67*, 790-798; d) S. Mishra, L. Unnikrishnan, S. K. Nayak, S. Mohanty, *Macromol. Mater. Eng.* **2019**, *304*, 1800463; e) S. Guerin, S. A. M. Tofail, D. Thompson, *NPG Asia Materials* **2019**, *11*, 10; f) D. Kim, S. A. Han, J. H. Kim, J.-H. Lee, S.-W. Kim, S.-W. Lee, *Adv. Mater.* **2020**, *32*, 1906989; g) R. Lay, G. S. Deijs, J. Malmström, *RSC Adv.* **2021**, *11*, 30657-30673.

[5] C. Park, K. Lee, M. Koo, C. Park, *Adv. Mater.* **2021**, *33*, 2004999.

[6] a) R. G. Kepler, in *Ferroelectric Polymers, Vol. 28* (Ed.: H. S. Nalwa), Marcel Dekker, INC, New York, **1995**, pp. 183-183; b) P. Martins, A. C. Lopes, S. Lanceros-Mendez, *Prog. Polym. Sci.* **2014**, *39*, 683-706.

[7] T. Jaworek, D. Neher, G. Wegner, R. H. Wieringa, A. J. Schouten, *Science* **1998**, *279*, 57-60.

[8] a) A. S. Tayi, A. Kaeser, M. Matsumoto, T. Aida, S. I. Stupp, *Nat. Chem.* **2015**, *7*, 281-294; b) O. Dumele, J. Chen, J. V. Passarelli, S. I. Stupp, *Adv. Mater.* **2020**, *32*, 1907247.

[9] O.-K. Kim, L.-S. Choi, H.-Y. Zhang, X.-H. He, S. Yan-Hua, *Thin Solid Films* **1998**, *327-329*, 172-175.
[10] a) S. I. Stupp, V. LeBonheur, K. Walker, L. S. Li, K. E. Huggins, M. Keser, A. Amstutz, *Science* **1997**, *276*, 384-389; b) G. N. Tew, L. Li, S. I. Stupp, *J. Am. Chem. Soc.* **1998**, *120*, 5601-5602; c) M. U. Pralle, K. Urayama, G. N. Tew, D. Neher, G. Wegner, S. I. Stupp, *Angew. Chem., Int. Ed.* **2000**, *39*, 1486-1489.
[11] a) R. Advincula, E. Aust, W. Meyer, W. Steffen, W. Knoll, *Polym. Adv. Technol.* **1996**, *7*, 571-576; b) A. Laschewsky, B. Mayer, E. Wischerhoff, X. Arys, P. Bertrand, A. Delcorte, A. Jonas, *Thin Solid Films* **1996**, *284-285*, 334-337.
[12] a) T. Goldacker, V. Abetz, R. Stadler, I. Erukhimovich, L. Leibler, *Nature* **1999**, *398*, 137-139; b) D. Ausserré, *Macromolecules* **2012**, *45*, 2478-2484.
[13] a) M. Fromel, E. M. Benetti, C. W. Pester, *ACS Macro Lett.* **2022**, *11*, 415-421; b) J. P. Nikolajsen, L. V. Thinnesen, O. A. Karabiber, K. Daasbjerg, S. U. Pedersen, M. Kongsfelt, M. Lillethorup, *ACS Appl. Polym. Mater.* **2023**, *5*, 3534-3541; c) G. J. Dunderdale, C. Urata, D. F. Miranda, A. Hozumi, *ACS Appl. Mater. Interfaces* **2014**, *6*, 11864-11868; d) T. Sato, G. J. Dunderdale, C. Urata, A. Hozumi, *Macromolecules* **2018**, *51*, 10065-10073.
[14] N. Schüwer, H. A. Klok, *Adv. Mater.* **2010**, *22*, 3251-3255.
[15] J. Wang, P. Karami, N. C. Ataman, D. P. Pioletti, T. W. J. Steele, H.-A. Klok, *Biomacromolecules* **2020**, *21*, 240-249.
[16] a) T. S. Kelby, W. T. S. Huck, *Macromolecules* **2010**, *43*, 5382-5386; b) J. Bünsow, J. Erath, P. M. Biesheuvel, A. Fery, W. T. S. Huck, *Angew. Chem., Int. Ed.* **2011**, *50*, 9629-9632.
[17] E. Spruijt, E.-Y. Choi, W. T. S. Huck, *Langmuir* **2008**, *24*, 11253-11260.
[18] J. Wang, H.-A. Klok, *Angew. Chem., Int. Ed.* **2019**, *58*, 9989-9993.
[19] S. Tugulu, P. Silacci, N. Stergiopulos, H.-A. Klok, *Biomaterials* **2007**, *28*, 2536-2546.
[20] a) M. Daglish, *Integr. Ferroelectr.* **1998**, *22*, 473-488; b) I. Lubomirsky, O. Stafsudd, *Rev. Sci. Instrum.* **2012**, *83*, 051101.
[21] a) J. O. Zoppe, N. C. Ataman, P. Mocny, J. Wang, J. Moraes, H.-A. Klok, *Chem. Rev.* **2017**, *117*, 1105-1318; b) W.-L. Chen, R. Cordero, H. Tran, C. K. Ober, *Macromolecules* **2017**, *50*, 4089-4113; c) J. Yan, M. R. Bockstaller, K. Matyjaszewski, *Prog. Polym. Sci.* **2020**, *100*, 101180.
[22] a) S. T. Milner, *Europhys. Lett.* **1988**, *7*, 695; b) A. Samadi, S. M. Husson, Y. Liu, I. Luzinov, S. M. Kilbey II, *Macromol. Rapid Commun.* **2005**, *26*, 1829-1834.
[23] M. Davis, D. Damjanovic, N. Setter, *J. Appl. Phys.* **2004**, *96*, 2811-2815.
[24] A. Stapleton, M. R. Noor, E. U. Haq, C. Silien, T. Soulimane, S. A. M. Tofail, *J. Appl. Phys.* **2018**, *123*, 124701.
[25] a) R. Kumar, B. G. Sumpter, S. M. Kilbey, II, *J. Chem. Phys.* **2012**, *136*, 234901; b) R. Zimmermann, J. F. L. Duval, C. Werner, J. D. Sterling, *Current Opinion in Colloid & Interface Science* **2022**, *59*, 101590.
[26] G. S. Manning, *Acc. Chem. Res.* **1979**, *12*, 443-449.
[27] a) N. Dingenouts, M. Patel, S. Rosenfeldt, D. Pontoni, T. Narayanan, M. Ballauff, *Macromolecules* **2004**, *37*, 8152-8159; b) Z. Ye, L. Li, F. Zhao, Y. Tian, Y. Wang, Q. Yang, L. Dai, X. Guo, *J. Polym. Sci., Part B: Polym. Phys.* **2019**, *57*, 738-747.
[28] Q. He, Y. Qiao, D. J. Mandia, S. Gan, H. Zhang, H. Zhou, J. W. Elam, S. B. Darling, M. V. Tirrell, W. Chen, *Langmuir* **2019**, *35*, 17082-17089.
[29] a) A. Jusufi, C. N. Likos, H. Löwen, *Phys. Rev. Lett.* **2001**, *88*, 018301; b) A. Jusufi, C. N. Likos, H. Löwen, *J. Chem. Phys.* **2002**, *116*, 11011-11027.
[30] K. P. Gregory, G. R. Elliott, H. Robertson, A. Kumar, E. J. Wanless, G. B. Webber, V. S. J. Craig, G. G. Andersson, A. J. Page, *PCCP* **2022**, *24*, 12682-12718.

[31] R. Kou, J. Zhang, T. Wang, G. Liu, *Langmuir* **2015**, *31*, 10461-10468.